

# Driving three atoms into singlet state in an optical cavity via adiabatic passage of dark state

Mei Lu<sup>1</sup>, Yan Xia<sup>1,2, \*</sup>, Jie Song<sup>3</sup>, and He-Shan Song<sup>2</sup>

<sup>1</sup>*Department of Physics, Fuzhou University, Fuzhou 50002, China*

<sup>2</sup>*School of Physics and Optoelectronic Technology,*

*Dalian university of Technology, Dalian 116024, China*

<sup>3</sup>*Department of Physics, Harbin Institute of Technology, Harbin 150001, China*

In this paper, we propose an efficient scheme to drive three atoms in an optical cavity into singlet state via adiabatic passage. Appropriate Rabi frequencies of the classical fields are selected to realize present scheme. The scheme is robust against the deviations in the pulse delay and laser intensity through some simple analysis of adiabatic condition. It is notable that the estimated range of effective adiabaticity condition coincides with the numerical results. When taking dissipation into account, we show that the process is immune to atomic spontaneous emission as the atomic excited states are never populated in adiabatic evolution. Moreover, under certain conditions, the cavity decay also can be efficiently suppressed.

## I. INTRODUCTION

The technique of adiabatic passage [1–3] has been proved as an effective coherently control dynamical process to realize quantum information processing (QIP) in many schemes [4–11]. Unlike the stimulated Raman adiabatic passage (STIRAP) where the Stokes pulse vanishes first, the two pulses vanish simultaneously while maintaining a constant finite ratio of amplitudes in f-STIRAP [12–14], which guarantees the creation of any pre-selected coherent superposition of ground states. A remarkable superiority of STIRAP and f-STIRAP is that if the evolution is adiabatic, the states of the system evolve within an adiabatic dark state subspace and the relevant states contain no contribution of the excited atomic states, so the spontaneous emission from excited states can be suppressed. Another advantage of adiabatic passage is the simpleness, for it needs not consider the precise tuning of pulse

---

\* E-mail: xia-208@163.com

areas, pulse widths, pulse shapes, pulse delay and detunings.

Cabello has proposed a special type of entangled state which is called  $N$ -particle  $N$ -level singlet states in 2002 [15]. These states are key solutions to many problems such as  $N$ -strangers, secret sharing and liar detection, which have no classical solutions. It has been shown that some types of supersinglets may violate the local hidden theory [16] and can be used to construct decoherence-free subspaces (DFSs), which are robust against collective decoherence [17]. Nevertheless, the generation of these states for  $N = 3$  which have the form

$$\frac{1}{\sqrt{6}}(|012\rangle - |102\rangle - |210\rangle + |120\rangle + |201\rangle - |021\rangle), \quad (1)$$

is still a problem both in theory and experiment. Here  $|0\rangle$ ,  $|1\rangle$  and  $|2\rangle$  represent three ground states. Jin *et al.* have proposed a scheme of generating a supersinglet of three three-level atoms in microwave cavity QED based on the resonant atom-cavity interaction [18]. The scheme is sensitive to the loss of cavity since the three atoms are sequentially sent through three different cavities and cavity fields which act as memories. Lin *et al.* also have raised a protocol for the preparation of a singlet state with three atoms via Raman transitions [19]. However, there will be a considerable influence caused by the cavity decay and spontaneous emission of the atoms. Shao *et al.* have put forward an approach by converting two-atom singlet state into three-atom singlet state via quantum Zeno dynamics [20], which needs to control the interaction time exactly.

To overcome these problems in Refs. [18–20], we propose a scheme where the state of the system evolves within a dark-state subspace via adiabatic passage. Three Gaussian shape pulses are used to complete the scheme and by this way the two Rabi frequencies of the laser fields maintain a constant finite ratio of amplitudes to get the desired final singlet states. Also sufficient adiabaticity can be achieved by choosing such pulses, for the estimates based on simple analysis of adiabaticity condition show the scheme is robust against deviations such as the pulse delay and pulse intensity, and the analysis is also validated by numerical calculation. Moreover, we also analyze the influence of the choice of laser intensity on the dissipation and achieve a relative high fidelity by choosing appropriate parameters.

The paper is organized as follows. In section II, we introduce the models for adiabatic passage and the pulses to realize the scheme. In section III, we discuss the robustness of parameters mismatch and dissipation due to the atomic spontaneous emission and cavity delay. Section IV contains the concluding remarks.

## II. GENERATION OF THREE-ATOM SINGLET STATE

As depicted in Fig. 1, three four-level atoms with tripod configuration are trapped in a bimodal vacuum cavity field. Each atom has an excited state  $|e\rangle$  and three ground states  $|f_L\rangle$ ,  $|f_R\rangle$  and  $|r\rangle$ . Supposed that the transition between the levels  $|e\rangle_i \leftrightarrow |f_L\rangle_i(|f_R\rangle_i)$  ( $i = 1, 2, 3$ ) is resonantly coupled to the cavity mode with the coupling strength  $g_{iL}(g_{iR})$  and the transition  $|e\rangle_i \leftrightarrow |r\rangle_i$  is resonantly driven by the classical pulse with the Rabi frequency  $\Omega_i$ . In the interaction picture, the Hamiltonian for the whole system can be written as ( $\hbar = 1$ )

$$\begin{aligned}
 H_{tot} &= H_l + H_c, \\
 H_l &= \sum_{i=1}^3 \Omega_i (|e\rangle_i \langle r| + |r\rangle_i \langle e|), \\
 H_c &= \sum_{i=1}^3 g_{iL} (a_L |e\rangle_i \langle f_L| + a_L^\dagger |f_L\rangle_i \langle e|) + g_{iR} (a_R |e\rangle_i \langle f_R| + a_R^\dagger |f_R\rangle_i \langle e|), \quad (2)
 \end{aligned}$$

where  $a_L^\dagger(a_R^\dagger)$  and  $a_L(a_R)$  are the creation and annihilation operations for the left(right)-circular polarization cavity mode, respectively. We assuming  $g_{iL} = g_{iR} = g$ ,  $\Omega_2(t) = \Omega_3(t) = \Omega(t)$ , and  $\Omega_1(t)$  to be real in the present paper for simplicity, the whole system will evolve in the following closed subspace:

$$\begin{aligned}
 |\phi_1\rangle &= |rf_Lf_R\rangle_{123}|00\rangle_{a_La_R}, \quad |\phi_2\rangle = |rf_Rf_L\rangle_{123}|00\rangle_{a_La_R}, \\
 |\phi_3\rangle &= |f_Lrf_R\rangle_{123}|00\rangle_{a_La_R}, \quad |\phi_4\rangle = |f_Rrf_L\rangle_{123}|00\rangle_{a_La_R}, \\
 |\phi_5\rangle &= |f_Lf_Rr\rangle_{123}|00\rangle_{a_La_R}, \quad |\phi_6\rangle = |f_Rf_Lr\rangle_{123}|00\rangle_{a_La_R}, \\
 |\phi_7\rangle &= |ef_Lf_R\rangle_{123}|00\rangle_{a_La_R}, \quad |\phi_8\rangle = |ef_Rf_L\rangle_{123}|00\rangle_{a_La_R}, \\
 |\phi_9\rangle &= |f_Lef_R\rangle_{123}|00\rangle_{a_La_R}, \quad |\phi_{10}\rangle = |f_Ref_L\rangle_{123}|00\rangle_{a_La_R}, \\
 |\phi_{11}\rangle &= |f_Lf_Re\rangle_{123}|00\rangle_{a_La_R}, \quad |\phi_{12}\rangle = |f_Rf_L e\rangle_{123}|00\rangle_{a_La_R}, \\
 |\phi_{13}\rangle &= |f_Lf_Lf_R\rangle_{123}|10\rangle_{a_La_R}, \quad |\phi_{14}\rangle = |f_Lf_Rf_L\rangle_{123}|10\rangle_{a_La_R},
 \end{aligned}$$

$$\begin{aligned}
|\phi_{15}\rangle &= |f_R f_L f_L\rangle_{123} |10\rangle_{a_L a_R}, \quad |\phi_{16}\rangle = |f_R f_R f_L\rangle_{123} |01\rangle_{a_L a_R}, \\
|\phi_{17}\rangle &= |f_R f_L f_R\rangle_{123} |01\rangle_{a_L a_R}, \quad |\phi_{18}\rangle = |f_L f_R f_R\rangle_{123} |01\rangle_{a_L a_R},
\end{aligned} \tag{3}$$

the subscripts 1, 2, 3,  $a_L$  and  $a_R$  represent atom 1, atom 2, atom 3, left-circular cavity mode and right-circular cavity mode, respectively.

There are six dark states with null eigenvalue in this subspace. We orthogonalize these states and get a special dark state  $|S\rangle$  which will evolve into an independent subspace while other states remain unchanged. This state can be expressed as

$$\begin{aligned}
|S\rangle = \frac{1}{N} &\left[ -\Omega(t)g(|\phi_1\rangle - |\phi_2\rangle) - \frac{\Omega_1(t)g}{2}(|\phi_3\rangle - |\phi_4\rangle - |\phi_5\rangle + |\phi_6\rangle) \right. \\
&\left. + \frac{\Omega_1(t)\Omega(t)}{2}(|\phi_{13}\rangle - |\phi_{14}\rangle - |\phi_{16}\rangle + |\phi_{17}\rangle) \right],
\end{aligned} \tag{4}$$

where  $N = \sqrt{\Omega_1^2(t)g^2 + 2\Omega^2(t)g^2 + \Omega_1^2(t)\Omega^2(t)}$ . Note that the state in Eq. (4) contains no contribution from the atomic excited states [21, 22], which can be considered as unpopulated during the whole interaction process, if the evolution is adiabatic. When the system is initially in the state

$$|\phi_i\rangle = \frac{1}{\sqrt{2}}(|\phi_1\rangle - |\phi_2\rangle), \tag{5}$$

under the condition

$$g \gg \Omega_1(t), \Omega(t), \tag{6}$$

and the Rabi frequencies following such behaviour

$$\lim_{t \rightarrow -\infty} \frac{\Omega_1(t)}{\Omega(t)} = 0, \quad \lim_{t \rightarrow +\infty} \frac{\Omega_1(t)}{\Omega(t)} = \tan \alpha, \tag{7}$$

we have an approximate evolution process from the initially entangled state  $|\phi_i\rangle$  to three-atom singlet state

$$|\phi_t\rangle = \frac{1}{\sqrt{6}}(|\phi_1\rangle - |\phi_2\rangle + |\phi_3\rangle - |\phi_4\rangle - |\phi_5\rangle + |\phi_6\rangle), \tag{8}$$

when  $\alpha = \arctan 2$ , which is the result we need. Let us define that  $\theta(t) = \arctan[\Omega_1(t)/\Omega(t)]$ , note that the rate of the change of the mixing angle  $\theta(t)$  must be much smaller compared to

the smallest separation  $\Delta\omega(t)$  of the corresponding eigenvalues [1, 12], the specific expression is

$$|\dot{\theta}(t)| \ll \Delta\omega(t). \quad (9)$$

Under these conditions, the evolution is adiabatic, and the system will remain in the dark state  $|S\rangle$ .

Next we discuss the Rabi frequencies and other correlative parameters that make the scheme experimentally feasible. We use three time-dependent pulses as follows

$$\begin{aligned} \Omega_1(t) &= \sin \alpha \Omega_0 \exp^{-(t-\tau)^2/T^2}, \\ \Omega(t) &= \cos \alpha \Omega_0 \exp^{-(t-\tau)^2/T^2} + \Omega_0 \exp^{-(t+\tau)^2/T^2}, \end{aligned} \quad (10)$$

and the variation of the two time-dependent Rabi frequencies  $\Omega_1$  (red dashed curve) and  $\Omega$  (blue solid curve) of lasers for atoms is shown in Fig. 2(a). By choosing  $\tau = 60/g$ ,  $T = 80/g$ ,  $\Omega_0 = 0.2g$ , we can see that when  $t \geq 100/g$ , the two Rabi frequencies are approximate to meet the relation  $\Omega_1 \simeq \frac{1}{2}\Omega$ . Thus the initial state  $|\phi_i\rangle$  will transfer into the target state  $|\phi_t\rangle$ . Fig. 2(b) shows the time evolution of the populations of the components of the state  $|S\rangle$   $P_1(P_2)$  (green dashed curve),  $P_3(P_4, P_5, P_6)$  (purple dotted curve) and  $P_{13}(P_{14}, P_{16}, P_{17})$  (red solid curve), respectively.

It is obvious that the population is almost completely transferred from the state  $|\phi_i\rangle$  to the state  $|\phi_t\rangle$  without populating other states during the dynamical process, which means the influence of the atomic spontaneous emission is effectively suppressed. For the density matrix of the two entangle states  $\rho_1, \rho_2$ , the Bures fidelity can be defined as [23]

$$F = \left( \text{tr} \sqrt{\rho_1^{1/2} \rho_2 \rho_1^{1/2}} \right)^2, \quad (11)$$

The relation between the fidelity and the evolution time  $t$  is shown in Fig. 2(c). When  $T = 100/g$ , the fidelity of the three-single state is 0.9996, which means we finally realize an almost perfect target state. Note that we need not control the time accurately since a fidelity  $F$  higher than 0.8775 can be obtain when  $t \geq 20/g$ .

### III. ADIABATICITY CONDITION AND NUMERICAL ANALYSIS

Now we come to discuss the conditions that a system with the initial state  $|\phi_i\rangle$  evolves adiabatically into the target state  $|\phi_t\rangle$ . In our analysis of the robustness of adiabatic passage

against variations in the experimental parameters, we start with the adiabatic condition (9). For the restrictive conditions of Eq. (6) and the given pulse shapes we have

$$\begin{aligned}
\dot{\theta}(t) &= \frac{4\tau}{T^2} \frac{\xi(t) \sin \alpha}{\sin^2 \alpha + [\cos \alpha + \xi(t)]^2}, \\
\Delta\omega(t) &= \sqrt{\frac{3g^2}{2} - \frac{\sqrt{9g^4 + 2g^2[\Omega_1^2(t) - \Omega^2(t)] + [\Omega_1^2(t) - \Omega^2(t)]^2}}{2} + \frac{\Omega_1^2(t)}{2} + \frac{\Omega^2(t)}{2}} \\
&\simeq \sqrt{\frac{\Omega_1^2(t)}{3} + \frac{2\Omega^2(t)}{3}} \\
&= \Omega_0 e^{-(t-\tau)^2/T^2} \sqrt{\frac{\sin^2 \alpha}{3} + \frac{2}{3}[\cos \alpha + \xi(t)]^2} = \Omega_{eff}(t),
\end{aligned} \tag{12}$$

where  $\xi(t) = e^{-4\tau t/T^2}$ . Then a limit for the pulse delay can be get by analysing the upper expressions.

We know that non-adiabatic conditions are most likely to occur when  $\dot{\theta}(t)$  reaches a maximum, that is  $\xi(t_0) = 1$ . Take  $t_0 = 0$  for example, then Eq. (12) is equal to

$$\begin{aligned}
\dot{\theta}(t_0) &= \dot{\theta}_{max}(t) = \frac{2\tau}{T^2} \tan \frac{1}{2}\alpha, \\
\Omega_{eff}(t_0) &= \Omega_0 e^{-\tau^2/T^2} \sqrt{\frac{\sin^2 \alpha}{3} + \frac{2}{3}(\cos \alpha + 1)^2}.
\end{aligned} \tag{13}$$

The maximum of  $\dot{\theta}(t)$  increases with  $\tau$  (see Eq. (13)), while  $\Omega_{eff}(t_0)$  is not necessarily the maximum of  $\Omega_{eff}(t)$ . To reach the adiabatic conditions (9) we must have  $\Omega_{eff}(t_0) \geq n\dot{\theta}(t_0)$ , where  $n$  is a ‘sufficiently large’ number and the choice of which depends on how much non-adiabaticity can be allowed. Then we find an upper bound on  $\tau$ ,

$$\Omega_0 T \geq \frac{2n\tau}{T} \frac{\tan \frac{1}{2}\alpha}{\sqrt{\frac{\sin^2 \alpha}{3} + \frac{2}{3}(\cos \alpha + 1)^2}} e^{\tau^2/T^2}. \tag{14}$$

We can see that the Rabi frequency needs to increase exponentially with  $\tau$  to suppress the non-adiabatic transitions.

Note that both  $\dot{\theta}(t)$  and  $\Omega(t)$  are pulse-shaped, it is convenient to find their full widths at half maximum(FWHM) for the following discussions.

$$T_{\dot{\theta}} \simeq \frac{T^2}{\tau} \ln \left( \sqrt{1 + \cos^2 \frac{1}{2}\alpha} + \cos \frac{1}{2}\alpha \right),$$

$$T_{\Omega} \simeq 2\tau + 2T\sqrt{\ln 2}. \quad (15)$$

When  $\tau \rightarrow 0$ , the pulses of  $\dot{\theta}(t)$  will be broaden and get broader than  $\Omega(t)$ . Then condition (9) will be violated in the early time and late time during the evolution. This problem can be solved by controlling the width of  $\dot{\theta}(t)$  smaller than the width of  $\Omega(t)$ , that is  $T_{\dot{\theta}} \leq T_{\Omega}$ . Then we obtain a lower bound for  $\tau$ . When  $\alpha = \arctan 2$  it reads as

$$\tau \geq 0.25T. \quad (16)$$

From the above analyses we can see that although for any sufficiently strong laser pulse and delay  $\tau > 0$  the f-STIRAP should work, there exists a more accurate adiabatic condition. For  $n = 5$ , the range is  $0.25T \leq \tau \leq 0.97T$  for  $\Omega_0 T = 12$ ,  $0.25T \leq \tau \leq 1.06T$  for  $\Omega_0 T = 16$  and  $0.25T \leq \tau \leq 1.13T$  for  $\Omega_0 T = 20$ . We also plot the relationship of the fidelity  $F$  versus the ratio  $\tau/T$  in the situation that  $\Omega_0 T = 12$  (blue dotted curve),  $\Omega_0 T = 16$  (green solid curve) and  $\Omega_0 T = 20$  (red dashed curve) by solving the master equation numerically in Fig. 3(a). The figure coincides with the results we deduce from Eq. (9) almost perfectly, which verifies that the adiabaticity is most easily achieved under the range we obtain. Fig. 3(a) also implies that for a particular value of  $\Omega_0 T$ , there exists a relative wide range of  $\tau/T$ , which means that our protocol is robust against the pulse delay in practical experiment. Fig. 3(b) shows the change of the time dependence of the smallest separation  $\Delta\omega(t)$  (blue dotted curve), the simplified smallest separation  $\Omega_{eff}(t)$  (green solid curve) and the mixing angle  $\theta(t)$  (red dashed curve) with the chosen parameters, which implies that the parameters our scheme chooses fit condition (9) well.

In all the above discussions, we have not considered any dissipation and assume the system does not interact with the environment. However, the system will interact with the environment inevitably which has influence on the availability of our scheme. Hence we will focus on discussing the influence of dissipation induced by the atomic spontaneous emission and the cavity decay. When we consider decoherence, the master equation of motion for the density matrix of the whole system can be expressed as

$$\begin{aligned} \dot{\rho} = & -i[H_{tot}, \rho] - \frac{\kappa_L}{2}(a_L^\dagger a_L \rho - 2a_L \rho a_L^\dagger + \rho a_L^\dagger a_L) \\ & - \frac{\kappa_R}{2}(a_R^\dagger a_R \rho - 2a_R \rho a_R^\dagger + \rho a_R^\dagger a_R) \end{aligned}$$

$$- \sum_{k=1}^3 \sum_{m=f_L, r, f_R} \frac{\Gamma_{em}^k}{2} (\sigma_{em}^k \sigma_{me}^k \rho - 2\sigma_{me}^k \rho \sigma_{em}^k + \rho \sigma_{em}^k \sigma_{me}^k), \quad (17)$$

where  $\Gamma_{em}^k$  is the spontaneous emission rate from the excited state  $|e\rangle$  to the ground states  $|m\rangle$  ( $m = f_L, r, f_R$ ) of the  $k$ th atom.  $\kappa_L(\kappa_R)$  is the decay rate of the left(right)-circular cavity mode. We assume  $\Gamma_{em}^k = \Gamma = \Gamma_0/3$  and  $\kappa_L = \kappa_R = \kappa$  for simplicity. Fig. 4 shows the relationships of the fidelity  $F$  versus the ratios  $\Omega_0/g$  and  $\Gamma/g$ ,  $\Omega_0/g$  and  $\kappa/g$ , respectively. The spontaneous emission rate makes a slighter influence on  $F$  under a larger laser intensity while cavity decay causes an opposite situation. The physical mechanism behind the behavior of the former case is just the adiabatic condition (9), which is satisfied better along with laser intensity increasing. That means under a relative large laser intensity, i.e. at  $\Omega_0/g = 0.3$  in Fig.4., the passage is more likely to evolve within the adiabatic dark state subspace which does not involve the excited atomic state  $|e\rangle$ . Therefore, the dissipation caused by atomic spontaneous emission decreases. However the populations of states where the cavity field are excited increase with laser intensity according to Eq. (4), which increase the dissipation caused by cavity decay finally. In such a way, the change of laser intensity decreases one error source while increasing another. So an appropriate value  $\Omega_0$  should be chosen when taking both the two factors into account. We also plot the relationship of the fidelity  $F$  versus the ratios  $\kappa/g$  and  $\Gamma/g$  by solving the master equation numerically in Fig. 5. Therefore we can see that under certain conditions both atomic spontaneous emission and cavity decay have a slight influence in fidelity  $F$ , since for a large atomic spontaneous emission  $\Gamma/g = 0.05$  and cavity decay  $\kappa/g = 0.05$ , the fidelity is still about 0.9244. Therefore our scheme is robust against the two error sources and achieve a superior result in theory.

Finally, we give a brief discussion about the basic factors for the experimental realization. The atomic configuration might be achieved in cesium atoms in our scheme. The state  $|r\rangle$  corresponds to  $F = 4, m = 3$  hyperfine state of  $6^2S_{1/2}$  electronic ground state,  $|f_L\rangle$  corresponds to  $F = 3, m = 2$  hyperfine state of  $6^2S_{1/2}$  electronic ground state,  $|f_R\rangle$  correspond to  $F = 3, m = 4$  hyperfine state of  $6^2S_{1/2}$  electronic ground state,  $|e\rangle$  corresponds to  $F = 4, m = 3$  hyperfine state of  $6^2P_{1/2}$  electronic state, respectively. In recent experimental condition [24, 25], the parameters  $g = 2\pi \times 750 MHz$ ,  $\Gamma_0 = 2\pi \times 2.62 MHz$ ,  $\kappa = 2\pi \times 3.5 MHz$  and the optical cavity mode wavelength in the range between 630 ~ 850 nm is predicted to achieve. By substituting the ratios  $\kappa/g = 0.0047$ ,  $\Gamma/g = 0.0035$  into Eq. (17), we will obtain a high fidelity of about 0.956, which shows our scheme to prepare three-atom singlet state



$|\phi_t\rangle$  is relatively robust against a realized one.

#### IV. CONCLUSION

In summary, we have proposed a scheme to generate a three-single state for three atoms trapped in an optical cavity via the adiabatic passage of dark state. The significant feature is that we need not to control the laser time exactly and it is robust against variations in the laser parameters such as pulse delay and laser intensity. So the scheme is robust, effective and simple. When considering dissipation, we can find that the protocol is robust against atomic spontaneous emission since the states evolve in a closed subspace where the atoms remain in the ground states in a adiabatic evolution. By choosing proper parameters, the scheme is also insensitive to cavity decay by numerical calculation intuitionally. The result shows that the scheme have a high fidelity and may be possible to implemented with the current experiment technology.

#### Acknowledgments

This work is supported by the funds from Education Department of Fujian Province of China under Grant No. JB08010, No. JA10009 and No. JA10039, the National Natural Science Foundation of Fujian Province of China under Grant No. 2009J06002 and No. 2010J01006, the National Natural Science Foundation of China under Grant No. 11047122 and No. 11105030, Doctoral Foundation of the Ministry of Education of China under Grant No. 20093514110009, and China Postdoctoral Science Foundation under Grant No. 20100471450.

- 
- [1] J. R. Kuklinski, U. Gaubatz, F. T. Hioe, and K. Bergmann, Phys. Rev. A **40**, 6741 (1989).
  - [2] U. Gaubatz, P. Rudecki, S. Schieman, and K. Bergmann, J. Chem. Phys. **92**, 5363 (1990).
  - [3] K. Bergmann, H. Theuer, and B. W. Shore, Rev. Mod. Phys. **70**, 1003 (1998).
  - [4] Z. Kis and F. Renzoni, Phys. Rev. A **65**, 032318 (2002).
  - [5] H. Goto and K. Ichimura, Phys. Rev. A **70**, 012305 (2004).
  - [6] S. B. Zheng, Phys. Rev. Lett. **95**, 080502 (2005).

- [7] X. Lacour, N. Sangouard, S. Gurin, and H. R. Jauslin, Phys. Rev. A **73**, 042321 (2006).
- [8] Z. J. Deng, K. L. Gao, and M. Feng, Phys. Rev. A **74**, 064303 (2006).
- [9] J. Song, Y. Xia and H. S. Song, J. Phys. B **40**, 4503 (2007).
- [10] Z. B. Yang, H. Z. Wu, and S. B. Zheng, Chin. Phys. B **19**, 094205 (2010).
- [11] J. Song, Y. Xia and H. S. Song, Appl. Phys. Lett. **96**, 071102 (2010).
- [12] N. V. Vitanov, K. A. Suominen, and B. W. Shore, J. Phys. B **32**, 4535 (1999).
- [13] M. Amniat-Talab, S. Gurin, N. Sangouard, and H. R. Jauslin, Phys. Rev. A **71**, 023805 (2005).
- [14] M. Amniat-Talab, S. Gurin, and H. R. Jauslin, Phys. Rev. A **72**, 012339 (2005).
- [15] A. Cabello, Phys. Rev. Lett. **89**, 100402 (2002).
- [16] N. D. Mermin, Phys. Rev. D **22**, 356 (1980).
- [17] A. Cabello, J. Mod. Opt. **50**, 10049 (2003).
- [18] G. S. Jin, S. S. Li, S. L. Feng, H. Z. Zheng, Phys. Rev. A **71**, 034307 (2005).
- [19] G. W. Lin, M. Y. Ye, L. B. Chen, Q. H. Du and X. M. Lin, Phys. Rev. A **76**, 014308 (2007).
- [20] X. Q. Shao, H. F. Wang, L. Chen, S. Zhang, Y. F. Zhao and K. Yeon, New. J. Phys. **12**, 023040 (2010).
- [21] A. S. Parkins, P. Marte, P. Zoller and H. J. Kimble, Phys. Rev. Lett. **71**, 3095 (1993).
- [22] T. Pellizzari, S. A. Gardiner, J. I. Cirac and P. Zoller, Phys. Rev. Lett. **75**, 3788 (1995).
- [23] R. Jozsa, J. Mod. Opt. **41**, 2315 (1994).
- [24] S. M. Spillane, T. J. Kippenberg, K. J. Vahala, K. W. Goh, E. Wilcut, and H. J. Kimble, Phys. Rev. A **71**, 013817 (2005).
- [25] J. R. Buck and H. J. Kimble, Phys. Rev. A **67**, 033806 (2003).

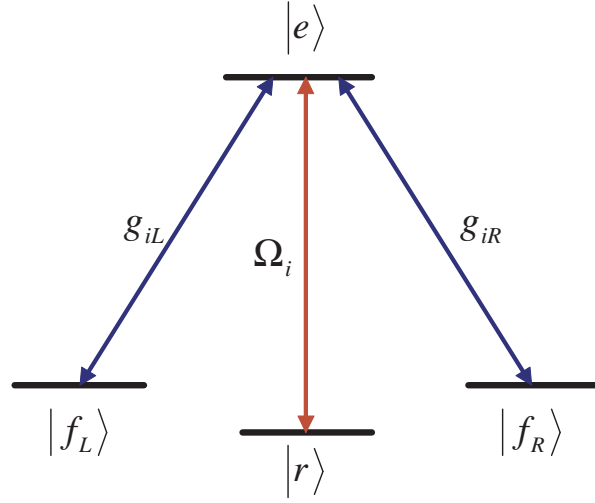
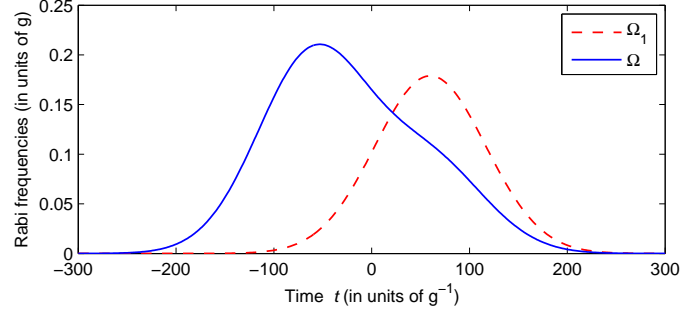
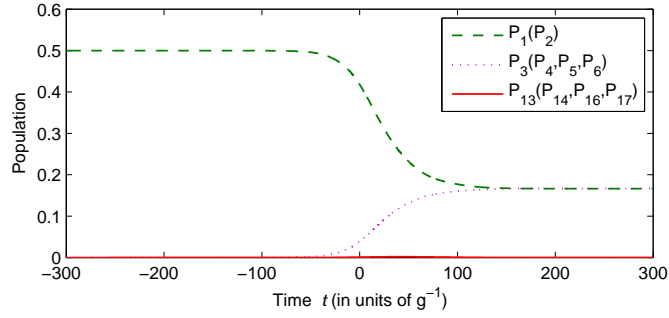


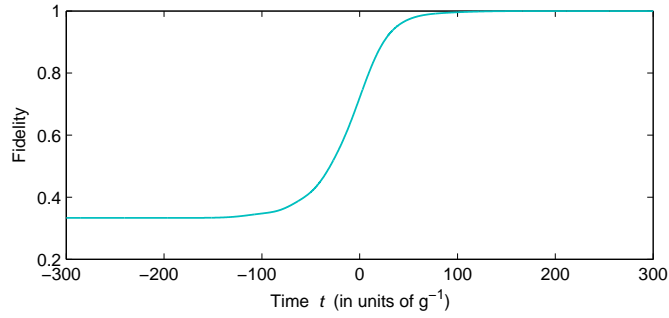
FIG. 1: The level configuration of the scheme. The transition  $|e\rangle \rightarrow |f_L\rangle$  and  $|e\rangle \rightarrow |f_R\rangle$  are coupled to left-circularly and right-circularly polarised cavity modes, respectively. A classical laser driver the transitions  $|r\rangle \rightarrow |e\rangle$ .



(a)

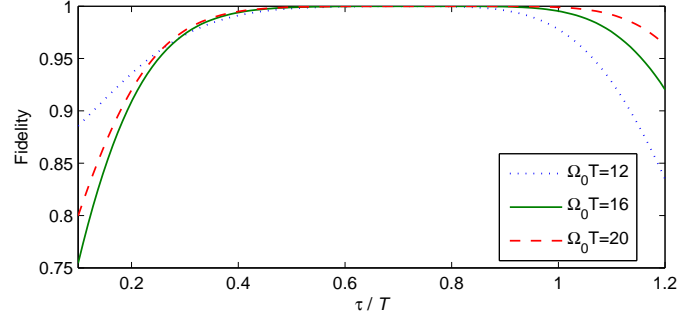


(b)

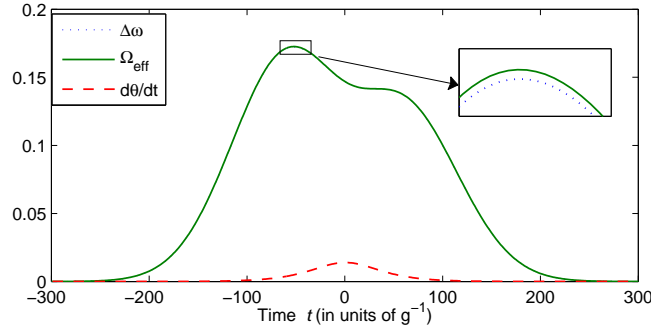


(c)

FIG. 2: (a) The time dependence of the laser fields for atoms. Here the red dashed curve and the blue solid curve represent the Rabi frequencies  $\Omega_1$  and  $\Omega$ , respectively. (b) Time evolution of the populations. Here the green dashed curve, the purple dotted curve and the red solid curve represent the populations  $P_1(P_2)$ ,  $P_3(P_4, P_5, P_6)$  and  $P_{13}(P_{14}, P_{16}, P_{17})$ , respectively. (c) Time evolution of the fidelity. We have chosen  $\tau = 60/g$ ,  $T = 80/g$ ,  $W_2/g = 100$ ,  $\Omega_0 = 0.2g$ .



(a)



(b)

FIG. 3: (a) The fidelity  $F$  vs. the ratio  $\tau/T$  when  $\Omega_0 T$  is in different values. Here the blue dotted curve, the green solid curve and the red dashed curve represent the values  $\Omega_0 T = 12, 16$  and  $20$ , respectively. (b) The time dependence of the the change of the smallest separation  $\Delta\omega$ , the simplified smallest separation  $\Omega_{eff}$  and the mixing angle  $\theta$ . Here the blue dotted curve, the green solid curve and the red dashed curve represent the change of  $\Delta\omega$ ,  $\Omega_{eff}$  and  $\theta$ , respectively. We have chosen  $\tau/g = 60$ ,  $W/g = 80$ ,  $\Omega_0/g = 0.2$ .

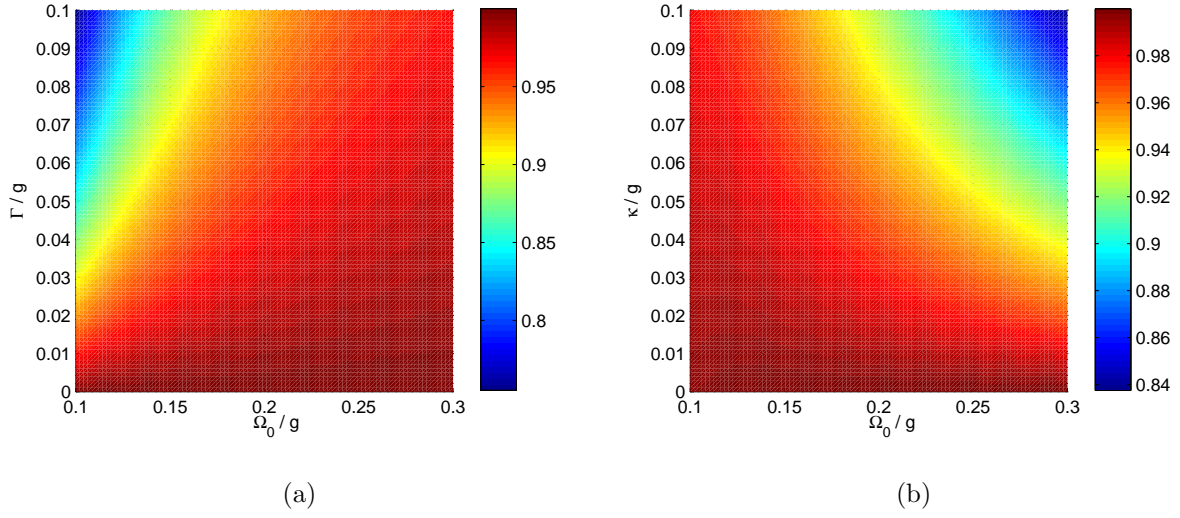


FIG. 4: (a) The fidelity  $F$  vs. the ratios  $\Omega_0/g$  and  $\Gamma/g$ . (b) The fidelity  $F$  vs. the ratios  $\Omega_0/g$  and  $\kappa/g$ .

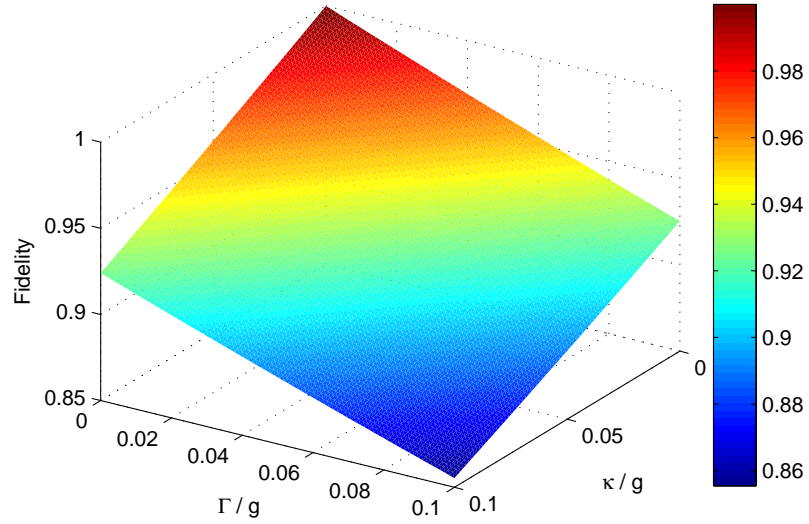


FIG. 5: The influence of ratios  $\kappa/g$  and  $\Gamma/g$  on the Fidelity  $F$  of the three-atom singlet state.